

# Development and In-Field Validation of Fungicide Nanoformulations of Prothioconazole and Tebuconazole and Modified Kraft Lignin

Silvio Vaz Júnior,\* Flávia Galarza, Gabriela Ciribelli Pompeu, Helliomar Pereira Barbosa, and Angelo Aparecido Barbosa Susse



Cite This: <https://doi.org/10.1021/acssuschemeng.4c09620>



Read Online

ACCESS |

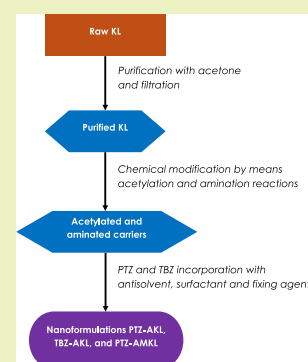
Metrics & More

Article Recommendations

Supporting Information

**ABSTRACT:** The search for alternatives to conventional agrochemicals presents itself as an excellent opportunity to develop sustainable, carbon-neutral agricultural technologies and to open new businesses. The use of kraft lignin, a renewable material with its chemical modification, is an opportunity to develop advanced and sustainable materials to reduce the negative impact of agrochemicals on the environment by reducing the active ingredient (AI) quantity for application. This work deals with the preparation, characterization, determination of incorporation efficiency (IE), and validation by in-field experiments of three fungicide nanoformulations using lignin-based carriers and prothioconazole (PTZ) and tebuconazole (TBZ) as AI at a mass ratio of 5 g of carrier: 600 mg of AI. The in-field experiments, associated with IE values from 83.2 to 100%, demonstrated the superior performances of the developed nanoformulations, against commercial formulations and isolated AI, to control Asian soybean rust and corn helminthosporiosis. In in-field experiments, the three formulations showed gains in productivity, highlighting PTZ-AMKL with 3030 kg ha<sup>-1</sup> for soybean and PTZ-AKL 6438 kg ha<sup>-1</sup> for corn, with productivity values above those obtained with commercial fungicide formulations—this behavior was observed also with the severity reduction in plants. Indeed, these new nanoformulations can reduce the quantities of both AI for pest control in order to reach sustainable agriculture by means of decreasing the negative effects from agricultural practices on the environment and public health.

**KEYWORDS:** *fungicides, acetylation, amination, corn crop, soybean crop*



## INTRODUCTION

In 2022, agrochemicals—as crop protection agents—reached a world market value of USD 78.72 billion, with this market expected to increase to USD 279.1 billion by 2024<sup>1</sup> due to the growth in demand for agricultural products. However, agrochemicals are one of the main classes of pollutants, with severe negative impacts on public health and the environment.<sup>2</sup> The search for alternatives to conventional agrochemicals presents itself as an excellent opportunity to develop sustainable, carbon-neutral agricultural technologies and open new businesses.<sup>3</sup>

According to Huang et al.,<sup>4</sup> triazole fungicides (TFs)—e.g., prothioconazole (PTZ) and tebuconazole (TBZ)—are systemic pesticides widely used in agriculture to prevent fungal diseases in vegetables, fruits, and crops. These fungicides are known for their high stability, moderate lipophilicity, and persistence in the environment, posing a risk to human health by disrupting endocrine function.<sup>5</sup> Thus, the reduction of their application concentrations is extremely beneficial to the environment and public health.

Carriers are organic and/or inorganic materials that serve for the incorporation, and subsequent release, of biologically active compounds, leading to an improvement in the effectiveness of

pharmaceutical and agrochemical formulations, which makes them a focus of great interest in academic and industrial research. Examples of these materials currently under study are clays, silicates, carbonates, metal hydroxides, cyclodextrin, chitosan, biochar, lignin, and synthetic polymers.<sup>6,7</sup> The desired characteristics for a given material to be used as a carrier for agrochemicals are biodegradability, biocompatibility, low toxicity, a simplified preparation process, promotion of slow release, and low mobility in soil.<sup>6</sup> Considering encapsulation as an example of a technological strategy related to carriers for agrochemicals, Hack et al.<sup>8</sup> observed that the development of controlled-release formulations of agrochemicals is still below expectations due to the substantial variation in the environmental conditions in which the capsules are applied. A few products that claim the controlled release (CR) of the active ingredient (AI) have made it to the market.

**Received:** November 21, 2024

**Revised:** February 26, 2025

**Accepted:** February 27, 2025

However, new or improved products can be achieved through encapsulation aimed at overcoming acute toxicity, instability, and incompatibility of actives, potentially generating value mainly attributed to nanoencapsulation.<sup>8</sup> Despite more than 10 years since publication, the limitations described by the authors remain challenging.

Regarding nanotechnology for agriculture, there is a generation of great opportunities for the advancement of knowledge and technological development, with the nanoformulations of agrochemicals (i.e., pesticides and fertilizers) being able to offer a CR to obtain complete biological efficacy without the risks of overdose.<sup>9</sup> And as observed by Wani et al.,<sup>10</sup> the nanoencapsulation of fertilizers, pesticides, fungicides, and herbicides ensures CR and targeted delivery of these agrochemicals required for efficient nutrient uptake, disease control, and enhanced growth of various plants and agricultural crops. Furthermore, nanotechnology, when applied to CR formulations, can contribute to the sustainable intensification of agricultural production systems.<sup>11,12</sup>

Lignin, a natural phenolic macromolecule which is commonly obtained as a residue of pulp and paper production, is one of the more promising materials for agrochemical carriers.<sup>13</sup> When using modified kraft lignin (KL), innovation is expected when compared to conventional applications,<sup>14</sup> which use an excess of the active ingredient, with increased cost and undesirable consequences for ecosystems.<sup>15</sup> An example of innovation is the use of hollow lignin nanospheres, with about 200 nm, developed for the slow release of drugs for cancer treatment, with an incorporation of 25% wt./wt. of the active principle facilitated by the surface area and by pore volume<sup>16</sup>—this approach can be used for agrochemicals. It is worth highlighting that the use of a natural and renewable phenolic macromolecule may improve the physicochemical properties involved in the incorporation of bioactive molecules—such as the availability and accessibility of interaction sites—through the formation of multilayer systems with H-bridge interactions and van der Waals forces.<sup>17</sup> It should be noted that lignin, as a constituent of lignocellulosic biomass, can be obtained from various sources, such as agricultural residues and wood kraft processing, at a low cost.<sup>18</sup>

According to Bajwa et al.,<sup>19</sup> lignin is the second most abundant natural material on the planet. Commercially, it is generated as waste from the production of paper and cellulosic ethanol. According to the same authors, world lignin production is approximately 100 million tons/year, valued at USD 732.7 million in 2015; and it is expected to reach USD 913.1 million by 2025, with a compound annual growth rate (CAGR) of 2%. Two main categories of lignin are lignosulfonate (~88%) and kraft lignin (~9%); however, a new category, organosolv (~2%), is gaining in popularity due to the production of second-generation biofuels.<sup>19</sup> Besides, Dessbesell et al.<sup>20</sup> observed that the KL recovery in pulp mills worldwide was 265,000 t in 2018. Furthermore, the application of lignin in agriculture as an encapsulating agent for pesticides has already been explored;<sup>21</sup> however, the strategy of structural modification of lignin to reach nanometric and micrometric scales is not frequent.

This work deals with the development and physicochemical characterization of three nanoformulations of PTZ and TBZ as AI using two renewable carriers obtained from the modification of KL by acetylation and amination reactions, respectively. Moreover, these three nanoformulations were

validated in in-field experiments to control fungal diseases in corn and soybean crops in the Brazilian Cerrado region.

The relevance of this study is because it can contribute to the sustainability of agriculture through the decrease in the negative effects of agricultural practices, i.e., pesticide application, on the environment and public health. Regarding innovation, we searched for nanoformulations with better performance than commercial formulations of PTZ and TBZ.

## MATERIALS AND METHODS

**Materials.** The industrial KL was kindly supplied by Suzano Paper and Cellulose from hybrid eucalyptus. All reagents and solvents used in the acetylation step (1,4-dioxane ( $\geq 99\%$ ), *N*-methylimidazolium ( $\geq 99\%$ ) and hydrochloric acid (37%)) and amination step (sodium hydroxide (97%), formaldehyde (37%), and ethylenediamine ( $\geq 99\%$ )) were of high-purity and supplied by Sigma-Aldrich without previous purification. Prothioconazole (PTZ; CAS number 178928-710-6) and tebuconazole (TBZ; CAS number 107534-96-3) — active ingredients (AI) of technical grade — were kindly supplied by Adama Brasil.

**Preparation of the Nanoformulations.** The KL acetylation route was adapted from the previous work of Thielemans and Wool<sup>22</sup> for KL esterification with unsaturated groups. Regarding the KL amination route, it was adapted from the previous work of Pang et al.<sup>23</sup> to produce nanoparticles of aminated alkaline lignin.

For the AI incorporation (PTZ and TBZ, separately), a mass ratio of 5 g of modified lignin (AKL and AMKL, separately) to 600 mg of AI was used based on an attempt to reduce drastically the mass of AI in each nanoformulation, when compared to the carrier mass; that is, a wt/wt ratio of 8.3 carrier: 1 AI; moreover, the dose of 600 mg L<sup>-1</sup> is an average dose obtained from the agronomic recommendation of different commercial fungicides composed of TBZ and PTZ. For all nanoformulations, ultrapure water (Milli-Q) was used as an antisolvent, sodium dodecyl sulfate (0.1 wt %/v, Sigma-Aldrich) as a surfactant, and polyvinylpyrrolidone (1 wt %/wt, Sigma-Aldrich) as a fixing agent. Thus, each nanoformulation was obtained as an emulsion.

Figure 1 illustrates the entire process of production for the nanoformulations PTZ-AKL, TBZ-AKL, and PTZ-AMKL.

The mass yield for each nanoformulation was calculated by using eq 1.

$$\text{Mass yield} = m_f / m_{\text{tf}} \times 100\% \quad (1)$$

Where  $m_f$  is the final mass obtained from the product and  $m_{\text{tf}}$  is the theoretical final mass, considering the modified lignins (AKL or AMKL) and the final products (PT-AKL, TBZ-AKL, and PTZ-AMKL).

**Characterization of the Nanoformulations.** First, purified KL, AKL, and AMKL carriers obtained from KL chemical modifications were chemically characterized by FTIR spectroscopy (Shimadzu IR Prestige-21 spectrometer, Shimadzu) for a wavenumber range of 4000 to 700 cm<sup>-1</sup> with a resolution of 4 cm<sup>-1</sup> and 32 scans, using KBr (Sigma-Aldrich) pellets at a mass ratio of 100 KBr: 1 sample.

Both carriers and purified KL were analyzed by <sup>31</sup>P NMR. The samples were prepared according to the methodology of Argyropoulos et al.<sup>24</sup> Initially, an aliquot (approximately 100 mg) of each sample was dried in a vacuum oven at 40 °C. The solvent solution was then prepared with a mixture in the proportion of 1.6:1 (v/v) of pyridine/deuterated chloroform [Sigma-Aldrich, purities  $\geq 99.0\%$  and 100%, 99.96 atom % D, contains 0.03% (v/v) TMS, respectively] in a 20 mL sample vial, with 5A molecular sieves. The internal standard solution was prepared in a 2 mL vial, using 10 mg of chromium(III) acetylacetonate (Sigma-Aldrich, purity 99.99% trace metals basis), 77.3 mg of cholesterol, and 286  $\mu\text{L}$  of solvent solution. Approximately 30 mg of each lignin was weighed into a 2 mL vial equipped with a stir bar, and 0.5 mL of the solvent solution and 100  $\mu\text{L}$  of the standard solution were added, leaving the mixture under constant stirring until complete solubilization (approximately 12 h). Then, 0.1 mL of

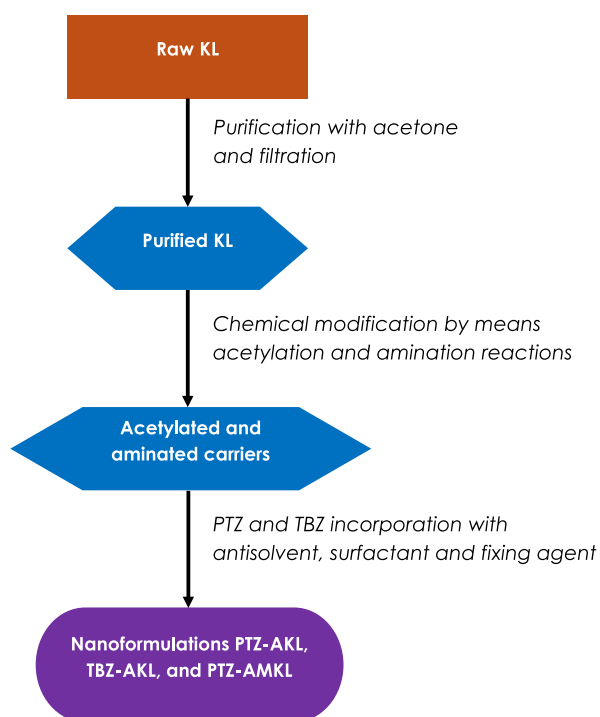


**Figure 1.** Experimental flowchart for the preparation of nanoformulations PTZ-AKL, TBZ-AKL, and PTZ-AMKL.

TMDP (Sigma-Aldrich, purity 99%) was added to the sample solutions with vigorous stirring. Finally, the sample solutions were transferred to an NMR tube and analyzed in resonance equipment of 600 MHz (Magna Ascend 600, Bruker), under pre-established conditions (Table S1).

The nanoformulations, initially composed of 5 g of carrier: 600 mg of AI, were physicochemically characterized by means of particle size, using the dynamic light scattering method (DLS, Malvern Panalytical), according to values previously defined by Ela et al.<sup>25</sup> for nanoparticles (200 nm); and by means of electrophoretic zeta potential (Zetasizer Advance, Malvern Panalytical), according to values previously defined by Pavan and Barron<sup>26</sup> for emulsion moderate stability ( $\pm 30$  to  $\pm 40$  mV).

The intermolecular interaction of AI and carrier, for each nanoformulation, was observed by means of fluorescence spectroscopy (RF-6000, Shimadzu) with an excitation range of 350–410 nm and an emission range of 420–550 nm.

**Determination of Incorporation Efficiency.** The incorporation efficiency (IE) describes the quantification of the AI molecule loading into the carrier molecule in order to form the physicochemical system AI-carrier for later release of the AI, and sometimes it is called encapsulation efficiency.<sup>27</sup>

For the nanoformulation TBZ-AKL, the IE was determined as follows based on an HPLC-PDA (Nexera, Shimadzu) analytical system. A Hypercarb chromatographic column (50 × 2.1 mm), with a particle size of 3  $\mu$ m; solvents: (i) mobile phase A:  $\text{H}_3\text{PO}_4$  (Sigma-Aldrich, ACS reagent with purity  $\geq 85\%$ ) 0.2% v/v, pH value adjusted with KOH (Sigma-Aldrich, ACS reagent with purity  $\geq 85\%$ ); (ii) mobile phase B: THF (Sigma-Aldrich, suitable for HPLC with purity  $\geq 99.9\%$ ); (iii) gradient: 0 min, 20% phase B; 3 min, 20% phase B; 4 min, 30% phase B; 15 min, 30% phase B; 20 min, 75% phase B; 22 min, 75% phase B; 22.1 min, 20% phase B; 30 min, 20% phase B. Flow rate: 0.5 mL  $\text{min}^{-1}$ ; PDA range: 200–600 nm; temperature of 50 °C; column oven: 80 °C; injection volume: 5  $\mu$ L. The calibration curve (Figure S1) was constructed with nine points (from 0.01–1.2 mg  $\text{mL}^{-1}$ ) using the TBZ Pestanal analytical standard (Supelco). We analyzed both the filtrate fraction (FF) and the gross fraction (GF) at  $t = 0$  and 48 h. The IE was determined by subtracting the fungicide rates present in the gross aliquot and in the filtered aliquot. The other

fractions collected at specific times ( $t = 1$  h,  $t = 2$  h,  $t = 4$  h,  $t = 8$  h,  $t = 24$  h, and  $t = 48$  h) were filtered in a Vivaspin 20 3 kDa (Merck) centrifugal concentrator, and the aqueous fractions were analyzed.

The IE was determined by eq 2, according to Machado et al.<sup>28</sup>

$$\text{IE}(\%) = \frac{m_i - m_f}{m_i} \times 100\% \quad (2)$$

For the nanoformulation PTZ-AKL, the IE was determined on the basis of an HPLC-PDA (Nexera, Shimadzu) analytical system. An Acclaim Mixed-Mode WAX-1 column (3.0 mm × 150 mm, 3  $\mu$ m) (Thermo Fisher Scientific) was used. Mobile phase 1: MeOH/ $\text{H}_2\text{O}$  1:1 (v/v) – phosphate buffer 0.05 mol  $\text{L}^{-1}$ , pH value of 3 (phosphoric acid and disodium hydrogen phosphate from Sigma-Aldrich, ACS reagent with purity  $\geq 85\%$  and 98.0–102.0%, respectively); mobile phase 2: acetone (Sigma-Aldrich, HPLC Plus with purity  $\geq 99.9\%$ ); injection volume of 5  $\mu$ L; flow rate of 0.45 mL  $\text{min}^{-1}$ ; column temperature of 45 °C; PAD range of 254 to 226 nm. The calibration curve (Figure S2) was constructed with seven points (from 0.01 to 0.24 mg  $\text{mL}^{-1}$ ) using PTZ Pestanal analytical standard (Supelco) diluted into ethyl acetate (Sigma-Aldrich, HPLC Plus with purity  $\geq 99.9\%$ ). The IE was calculated from eq 2.

According to the method used, samples of the filtrates collected at different times ( $t = 0$ ,  $t = 2$  h,  $t = 4$  h,  $t = 8$  h,  $t = 24$  h, and  $t = 48$  h) were injected, as well as an aliquot of the gross emulsion solution at times  $t = 0$  and  $t = 48$  h.

The presence of the AI PTZ was only detected in the raw aliquots at  $t = 0$  and 48 h. In the other aliquots of the filtrates, at other times, no signal related to the fungicide pattern was detected. In other words, the incorporation was high and remained stable over the 48-h period.

For the nanoformulation PTZ-AMKL, the IE was determined based on, again, an HPLC-PDA (Nexera, Shimadzu) analytical system. A Raptor ARC-18 column of 1.8  $\mu$ m, 150 mm × 2.1 mm (Restek); column oven temperature of 70 °C; PDA range of 210 to 500 nm; cell temperature of 45 °C. Mobile phase 1: 0.1% v/v aqueous formic acid (Supelco, LC-MS LiChropur with a purity of 80–100%) solution; mobile phase 2: acetonitrile (Supelco, suitable for LC/MS, LiChrosolv with purity of  $\geq 99.9\%$ ) and 0.1% v/v formic acid (Supelco, LC-MS LiChropur with purity of 80–100%). As for the last nanoformulation, PTZ Pestanal analytical standard (Supelco) was diluted into ethyl acetate (Sigma-Aldrich, HPLC Plus with purity  $\geq 99.9\%$ ). And the IE was calculated from eq 2.

According to the method used, samples of the filtrates collected at different times ( $t = 0$  h,  $t = 2$  h,  $t = 4$  h,  $t = 8$  h,  $t = 24$  h, and  $t = 48$  h) were injected, as well as an aliquot of the gross emulsion solution at time  $t = 0$  h.

**In-Field Validation Experiments.** The three nanoformulations obtained (PTZ-AKL, TBZ-AKL, and PTZ-AMKL), as emulsions, were intended for agronomic field experiments to control Asian soybean rust (caused by the fungus *Phakopsora pachyrhizi*) and to control corn helminthosporiosis (caused by the fungus *Exserohilum turcicum*). Both fungal diseases are of special concern for Brazilian crop producers in the Cerrado region, leading to losses in production and income.<sup>29,30</sup>

The in-field validation experiments were conducted according to previous Embrapa Cerrados's experience in the study of both fungal diseases.

To evaluate the control of corn helminthosporiosis, four experiments were conducted using the Agroceres 8088Pro2 (Agroceres) corn cultivar. In experiments 1 and 2, corn was sown in 290 mL tubes containing a commercial substrate (N, P, K, limestone, sphagnum peat moss, coconut fiber, rice hull, and sugar cane trash; Bioplant). Treatments were assigned in a completely randomized design with 7 and 12 replicates, respectively. The first three leaves fully expanded were sprayed with the nanoformulations. Following treatment, plants remained in the greenhouse for 48 h before being inoculated with a calibrated *E. turcicum* spore suspension ( $5 \times 10^4$  spores  $\text{mL}^{-1}$ ). Inoculated plants were maintained in a humid environment for 48 h. Ten days postinoculation, disease severity assessments via a diagrammatic scale (experiment 1) and lesion counts (experiments

1 and 2) were conducted. In experiment 1, commercial fungicides Tebufort (TBZ; commercial formulation from UPL) and FoxXpro (PTZ, bixafen, and trifluorostrobin; commercial formulation from Bayer) were used as positive controls. In experiment 2, the nanoformulation emulsions containing fungicides were tested.

Parallel to the greenhouse trials, two field experiments were established at the Embrapa Cerrados experimental field on January 31, 2023, and November 24, 2023. A basal fertilization rate of 300 kg ha<sup>-1</sup> of N–P–K (04-30-10) was applied, and chlorpyrifos (commercial formulation from Sumitomo Chemical) was used for pest management. The field study was set up in a randomized block design with five replicates, each comprising four rows of corn (6 m in length). Within each plot, five plants were evaluated in the central rows. Spraying was performed using a CO<sub>2</sub>-propelled sprayer with a 200 L ha<sup>-1</sup> flow rate, in the first field experiment on March 14, 2023. Disease incidence and severity assessments were conducted on March 31 and April 28, 2023. In the first assessment, all fully expanded leaves were examined for lesion counts and disease severity. In the second, only the leaf immediately below the ear was evaluated for lesion count and severity by using a diagrammatic scale. The second experiment was sprayed on December 26, 2023, assessed on January 31, 2024, and harvested on April 30, 2024.

To assess the efficacy of nanoformulations in controlling Asian soybean rust, two experiments were conducted using soybean cultivars BRS7981 (Embrapa) in greenhouse conditions and Soytech 700 I2X (BASF) in the field.

In the greenhouse trials, soybean seeds were sown individually in 290 mL tubes filled with commercial substrate. The plants were maintained in the greenhouse until the first trifoliolate leaf fully expanded, at which point they were treated with nanoformulations and commercial fungicides. Each treatment had six replicates arranged in a completely randomized design. The soybean plants were inoculated by spraying *Phakopsora pachyrhizi* spores (1 × 10<sup>6</sup> spores mL<sup>-1</sup>) suspension. After inoculation, the plants were maintained in a humid chamber for 48 h. Following a 15-day incubation, the trifoliolates were examined for rust lesions by using a stereoscopic microscope. Subsequently, the plants were returned to the greenhouse for a week. The first two leaves and the first trifoliolate were evaluated for lesion (pustule) count using a stereoscopic microscope.

Parallel to the greenhouse trial, a field experiment was established at the Embrapa Cerrados experimental field on January 30, 2023. A basal fertilization rate of 300 kg ha<sup>-1</sup> of N–P–K (04-30-10) was applied, and chlorpyrifos (commercial formulation from Sumitomo Chemical) was used for pest management. The field trials were arranged in a randomized block design with four replicates, each containing four rows of soybean plants (3.5 m in length). Applications were performed on March 5 and March 30, 2023, with assessments on April 13, 2023. In the evaluations, four plants were sampled per plot, and the severity of rust infection on all leaves was estimated by using a diagrammatic scale. The soybeans were harvested on July 23, 2023.

In all experiments, data were analyzed for variance. Where significant treatment effects were observed, Tukey's mean tests were applied at a 5% significance level, using SISVAR software (Federal University of Lavras).

## RESULTS AND DISCUSSION

**Characterization of the Nanoformulations.** Figure 2 depicts the FTIR analysis of the carriers, ALK and AMKL.

For better visualization and comparison of the results, the spectra were superimposed, highlighting the structural modifications after structural modification via the acetylation reaction. The main bands related to lignins (with or without modification) appear around 1516 cm<sup>-1</sup>, related to vibrations of the aromatic ring; at 1460 cm<sup>-1</sup>, vibrations of the aromatic structure and in-plane C–H deformation, O–H stretching at 3404 cm<sup>-1</sup>, C–O deformation at 1113 cm<sup>-1</sup>, and 1030 cm<sup>-1</sup> deformations in the aromatic C–H plane (guaiaacyls) and primary alcohols—these observations are in accordance with

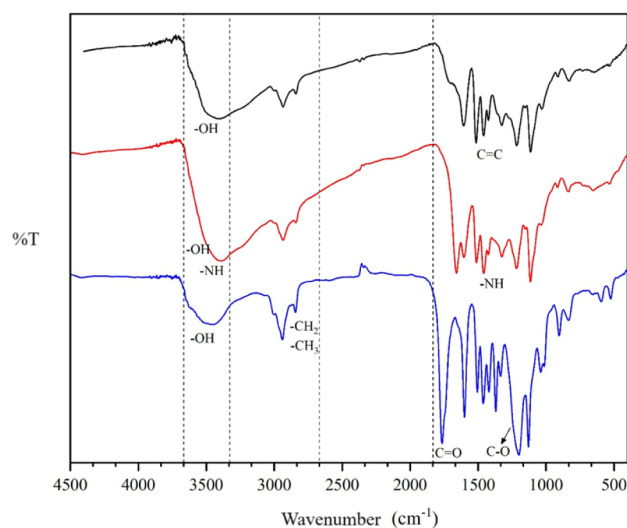


**Figure 2.** FTIR spectra of purified KL (black), AMKL (red), and AKL (blue), obtained with the KBr pellet at 4 cm<sup>-1</sup> of resolution.

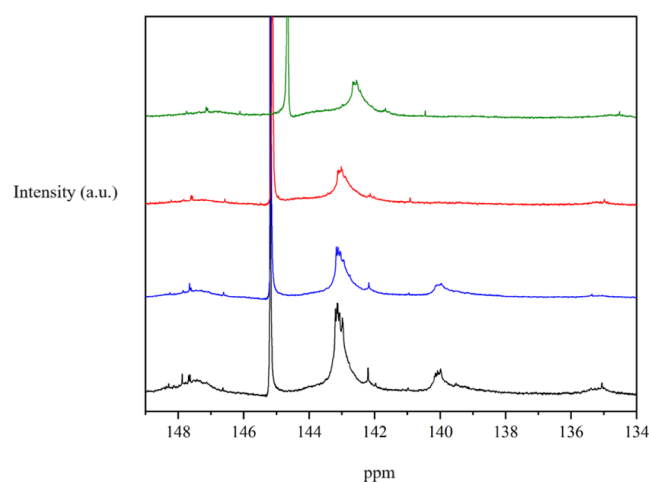


**Figure 3.** <sup>31</sup>P NMR spectra for raw KL (black), purified KL (blue), AKL (red), and AMKL carrier (green).

the scientific literature for FTIR applied to lignins characterization.<sup>31</sup> Comparing the spectra of KL and modified lignins (AMKL and AKL), the appearance of new bands related to the introduction of substitutions is observed. For amination, the chemical modification can be observed by the divided band in 1625 cm<sup>-1</sup> attributed to –NH<sub>2</sub> and to –NH. For acetylation, the chemical modification is observed, above all, by the insertion of acetyl groups, in 1768 and 1208–1127 cm<sup>-1</sup>, referring to the C=O stretching of carboxylic acids and to two bands of unsaturated ethers.

Figure 3 depicts the results from <sup>31</sup>P NMR analysis.

From Figure 3, it is possible to initially identify a gradual shift of the peaks, especially in the lignin samples with chemical modification. This variation in the position of the signals in the spectrum refers to changes in their structures that result in changes in the electronic environments of certain atoms, such as hydrogen or carbon, causing variations in the chemical shift.<sup>32</sup> Another observation to be made is the identification of typical signals for aliphatic (150–145 ppm), aromatic (145–137 ppm), and carboxylic (136–134 ppm) hydroxy groups, present in all lignin samples, but with different intensities. This implies the occurrence of available substitutions of hydroxyls

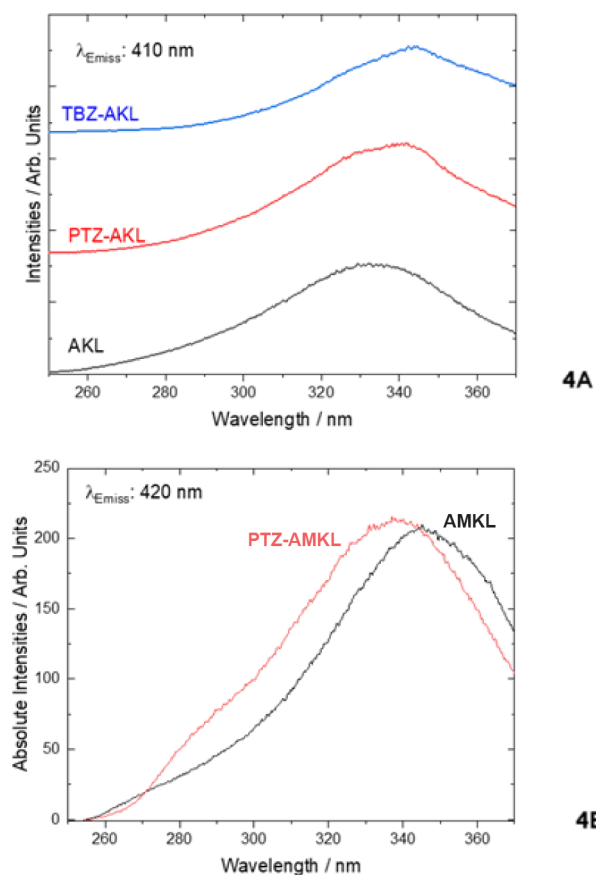


**Figure 4.** UV–vis fluorescence spectra in the excitation mode for emission at 410 nm (4A) and 420 nm (4B), recorded at room temperature.

before chemical modification by acetyl groups, in the acetylation reaction (AKL), and amine groups, in the amination reaction (AMKL).

Figures 4 and 5 present the fluorescence spectra of UV-vis fluorescence of the nanoformulations.

Excitation spectra were recorded covering the range of 250–370 nm, monitoring the emission wavelength at 410 nm. The excitation spectra exhibited a broad band in the range of 300–360 nm, with a slight shift toward longer wavelengths observed when comparing AKL to PTZ-AKL and TBZ-AKL (Figure 4A). This shift suggests significant modifications in the chemical environment of AKL due to the formation of chemical bonds with PTZ (or TBZ) (Figure 4B).

The excitation spectra of PTZ-AMKL and AMKL display a broad homogeneous band centered at 350 nm (Figure 4B). The addition of PTZ to the AMKL host results in the formation of a shoulder at approximately 290 nm, indicating that PTZ introduces a new energy transfer channel for intramolecular charge transfer in higher energy wavelengths.

Under excitation at 350 nm, the emission profiles of AKL, PTZ-AKL, and TBZ-AKL show similarities, but PTZ-AKL exhibits a higher intensity with a peak at around 420 nm (Figure 5A). This suggests that PTZ and TBZ positively influence the chemical environment of AKL, enhancing its emission bands. Additionally, shifts to longer wavelengths indicate an extension of the  $\pi$ -conjugated system and improved intramolecular charge transfer.<sup>33,34</sup> This mechanism suggests that the distribution of the electron cloud shifts toward these

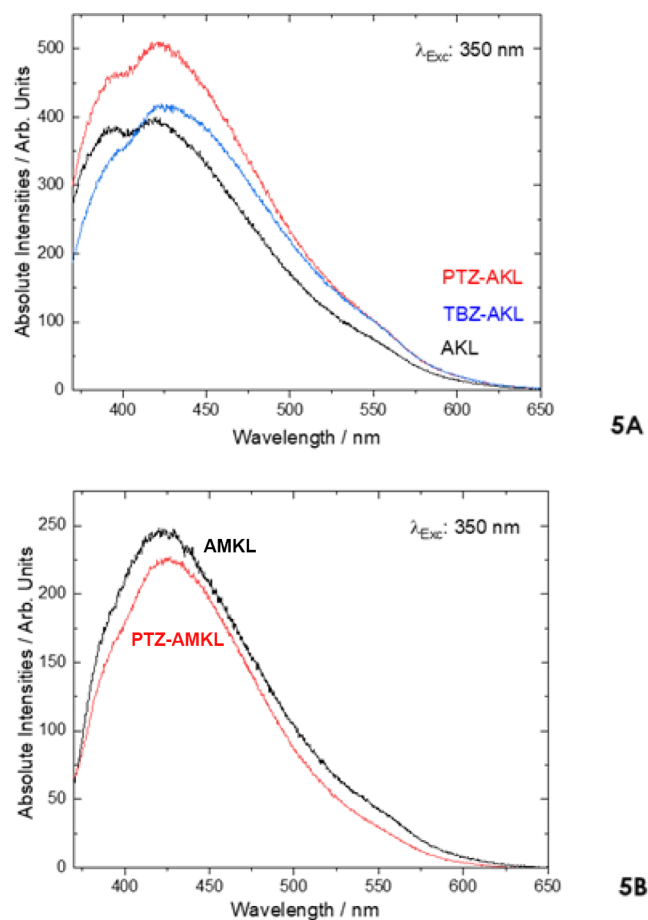


**Figure 5.** UV–vis fluorescence spectra in the emission mode of AKL, PTZ-AKL, and TBZ-AKL (5A) and PTZ-AMKL and AMKL (5B) in DMSO, under excitation at 350 nm, recorded at room temperature.

functional groups, thereby improving luminescence compared to unmodified AKL.

The emission spectra recorded from 370 to 650 nm exhibit significant luminescence quenching in PTZ-AMKL compared to that in AMKL (Figure 5B). Notably, the shoulder at approximately 550 nm in the AMKL emission band is suppressed in PTZ-AMKL, confirming that PTZ is responsible for eliminating this feature.

Table 1 presents the determined results for particle size and zeta potential (for emulsion stability evaluation) and mass yield, with their comparisons against technical references.

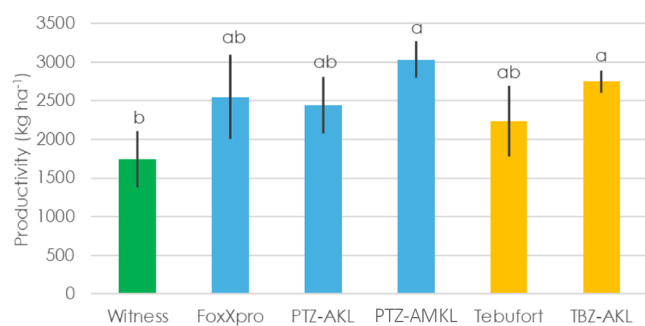
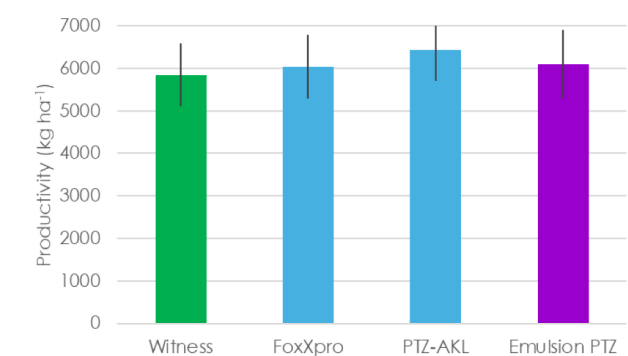
According to those reference values for the analytical parameters (particle size and zeta potential) and the process mass yield, the results presented in Table 1 are in accordance with the recognition of a stable nanoparticle/nanosystem.

**Determination of Incorporation Efficiency.** According to eq 2 applied to the experimental results from the HPLC-PAD methods, the following IE values for the three nanoformulations were determined: (i) 98.2% for PTZ-AKL; (ii) 100% for TBZ-AKL; (iii) 83.2% for PTZ-AMKL.

Taking into account the previous value determined by Machado et al.<sup>28</sup> of 73% for TBZ-modified lignin, our TBZ-AKL system showed more efficiency. For PTZ, Beckers et al.<sup>36</sup> produced PTZ-methacrylated lignin sulfonate with an encapsulated efficiency (or IE) of 77%. Additionally, Wang et al.<sup>37</sup> obtained a maximum efficiency of 95% for the fungicide

**Table 1. Physicochemical Characterization of the Nanoformulations**

Reference technical coefficient	Reference value	Scientific reference	Determined experimental value
Particle size	200 nm	25	168.48 ± 2.68 (PTZ-AMKL) 58.07 ± 0.49 (TBZ-AKL) 194.52 ± 0.59 (PTZ-AKL)
Colloidal stability, as zeta potential	± 30 to ±40 mV	26	−38.66 ± 0.72 (PTZ-AKL) −38.20 ± 5.83 (PTZ-AMKL) −32.45 ± 7.55 (TBZ-AKL)
Mass yield	83.1% wt./wt.	35	114% (PTZ-AMKL) 77% (TBZ-AKL) 91.2% (PTZ-AKL)

**Figure 6.** Soybean productivity, in kg ha<sup>−1</sup>, with the use of nanoformulations, commercial fungicides, and control. (Means followed by the same letter as not different according to Tukey's test at 0.05.)**Figure 7.** Corn productivity, in kg ha<sup>−1</sup>, and error bars with the use of nanoformulation, Fox Xpro fungicide, isolated PTZ, and control.

pyraclostrobin using a lignin/surfactin carrier. Thus, our nanoformulations proved to be suitably incorporation efficient.

These determined values indicated adequate behavior for the in-field release of the AI.

Regarding efforts to determine the release rate using dialysis for desorption (not shown), they were not conclusive. But we reached a release rate of nearly 40% 48 h<sup>−1</sup> for TBZ and nearly 84% 48 h<sup>−1</sup> for PTZ as indicators to be explored in a future step of scale-up. However, the proven in-field performances were more relevant—for this study—than the determination of the release rate in the laboratory because the performance is a mandatory parameter for the validation of the three nanoformulations.

**In-Field Validation Experiments.** Figures 6 and 7 show the results of productivity for soybean cultivation and corn cultivation, respectively.

In in-field experiments, the three formulations showed gains in productivity compared to the control, which is the area cultivated without the use of a fungicide. The same occurred

**Table 2. Means of Severity and Number of Lesions Per Leaf of Helminthosporiosis Inoculated on Corn and Control Efficiency Result from the Applications of Different Fungicides**

Treatments	Experiment 1					
	Number of lesions/leaf	Control (%)	Severity (%)	Reducing Severity (%)		
TBZ-AKL	1.83	a <sup>a</sup>	85	4.76	a	91
Tebuconazole	2.31	a	81	5.24	a	90
PTZ-AKL	2.55	a	79	13.21	a	76
PTZ-AMKL	3.20	a	73	20.76	a	62
Protrioconazole + trifloxystrobin + bixafen	3.97	a	67	24.03	a	56
Control	11.93	b	-	54.70	b	-
C.V. (%)	34.99			10.71		
Treatments	Experiment 2					
	Number of lesions/leaf	Control (%)				
TBZ-AKL	4.46	a	93			
Emulsion of TBZ	5.92	a	90			
PTZ-AKL	5.29	a	91			
PTZ-AMKL	9.75	a	84			
Emulsion of PTZ	5.15	a	92			
Control	60.83	b	-			
C.V. (%)	22.11					

<sup>a</sup>Means followed by the same letter as not different according to Tukey's test at 0.05; C.V. = coefficient of variation of plots.

for commercial products. However, the PTZ-AMKL and TBZ-AKL nanoformulations showed gains in productivity compared to the commercial products FoxXpro and Tebufort, respectively.

It can be observed that the PTZ-AMKL nanoformulation outperformed the FoxXpro fungicide by 482.5 kg ha<sup>−1</sup>, while the TBZ-AKL nanoformulation outperformed the Tebufort fungicide by 510 kg ha<sup>−1</sup> of soybean, providing a significant increase (Figure 6). In corn cultivation (Figure 7), the TBZ-AKL nanoformulation stands out, numerically surpassing the FoxXpro fungicide by 405.05 kg ha<sup>−1</sup>.

It is worth mentioning that, regarding PTZ associated with lignins in a nanosystem nanoformulation, Beckers et al.<sup>36</sup> developed nanocarriers from lignin sulfonates to incorporate PTZ without in-field validation. The same observation applies to TBZ, with Machado et al.<sup>28</sup> developing a lignin-based nanocarrier associated with TBZ without in-field validation.

In the corn greenhouse experiments, the formulations significantly reduced the disease compared with the control (Table 2). The TBZ-AKL formulation stood out, as it provided

**Table 3. Means of Incidence, Severity, and Number of Lesions per Leaf of Helminthosporiosis on Corn and Control Efficiency Resulting from the Applications of Different Fungicides, in Two Assessments, on the Field<sup>a</sup>**

Treatments	First assessment						
	Number of lesion/leaf	Control (%)	Incidence (%)	Reducing incidence (%)	Severity (%)	Reducing severity (%)	
PTZ-AKL	0.017 a	98	1.67 a	97	0.067 a	98	
Protiocoazole + trifloxystrobin + bixafen	0.097 a	88	8.33 a	84	0.271 a	92	
TBZ-AKL	0.141 a	82	14.06 a	73	0.609 a	83	
Tebuconazole	0.179 a	78	7.14 a	86	0.393 a	89	
PTZ-AMKL	0.221 a	72	17.65 a	66	0.610 a	83	
Control	0.797 b	-	51.56 b	-	3.539 b	-	
C.V. (%)	29.66		22.06		3.43		
Treatments	Second assessment						
	Number of lesion/leaf	Control (%)	Incidence (%)	Reducing incidence (%)	Severity (%)	Reducing severity (%)	
PTZ-AKL	1.50 a	84	60 a	40	3.85 a	90	
PTZ-AMKL	2.05 ab	78	79 ab	21	4.87 ab	88	
Protiocoazole + trifloxystrobin + bixafen	4.17 bc	56	100 b	0	13.64 ab	66	
Tebuconazole	4.39 c	53	94 b	6	15.78 ab	61	
TBZ-AKL	5.20 c	45	87 b	13	16.73 b	59	
Control	9.38 d	-	100 b	-	40.35 c	-	
C.V. (%)	26.45		12.58		9.31		

<sup>a</sup>Means followed by the same letter as not different according to Tukey's test at 0.05; C.V. = coefficient of variation of plots.

**Table 4. Means of Number of Lesions per Leaf of Asian Soybean Rust on Inoculated Soybean Plants and Control Efficiency Resulting from The Applications of Different Fungicides<sup>a</sup>**

Treatments	Number of lesions/leaf	Control (%)
PTZ	0.264 a	99.8
PTZ-AMKL	1.534 a	98.8
PTZ-AKL	5.068 a	96.2
TBZ-AKL	7.002 a	94.7
TBZ	7.666 a	94.2
Control	132.335 b	-
C.V. (%)	59.87	

<sup>a</sup>Means followed by the same letter as not different according to Tukey's test at 0.05; C.V. = coefficient of variation of plots.

greater control of the number of lesions and a greater reduction in severity than the other treatments. In the corn field experiments, the formulations reduced the number of lesions on the leaves, the incidence of symptomatic leaves, and the severity of helminthosporiosis, both in the first assessment and in the second assessment carried out 45 days after spraying, with the PTZ-AKL formulation standing out (Table 3). A significant increase in corn yield was observed with the

use of PTZ-AKL, surpassing the "PTZ + trifloxystrobin + bixafen" fungicide by 405.05 kg of ha<sup>-1</sup> (Figure 6).

The three formulations also significantly reduced the number of lesions of Asian soybean rust under greenhouse conditions (Table 4), with a reduction in the number of lesions of more than 94%. In the field, the PTZ-AMKL formulation stood out; as well as reducing severity by 52%, it led to a 74% increase in yield compared to the untreated control (Table 5). It can be observed that the PTZ-AMKL nanoformulation outperformed the "PTZ + trifloxystrobin + bixafen" fungicide by 482.5 kg ha<sup>-1</sup>, while the TBZ-AKL nanoformulation outperformed the TBZ fungicide by 510 kg ha<sup>-1</sup> of soybean.

## CONCLUSIONS

Three nanoformulations were successfully developed using chemically modified KL, through acetylation and amination reactions, as carriers and PTZ and TBZ as AI. These nanoformulations were validated in the control of fungal diseases in corn and soybean crops.

FTIR and <sup>31</sup>P NMR confirmed the chemical modifications to obtain AKL and AMKL carriers. UV-vis fluorescence confirmed the formation of nanoformulation systems by means of intermolecular interactions.

**Table 5. Means of Severity of Asian Soybean Rust, Control Efficiency, Yield, and Increased Yield Resulting from the Applications of Different Fungicides<sup>a</sup>**

Treatments	Severity (%)	Control (%)	Yield (kg ha <sup>-1</sup> )	Increasing yield (%)
LKAM-PTZ	17.85 a	52	3030.00 a	74
TBZ-AKL	23.19 ab	37	2747.50 a	58
Tebuconazole	29.77 bc	19	2237.50 ab	28
Protiocoazole + trifloxystrobin + bixafen	29.93 bc	19	2547.50 ab	46
PTZ-AKL	32.26 bc	13	2445.00 ab	40
Control	36.89 c	-	1742.50 b	-
C.V. (%)	20.56		16.43	

<sup>a</sup>Means followed by the same letter as not different according to Tukey's test at 0.05; C.V. = coefficient of variation of plots.

Finally, IE values ranged from 83.2 to 100%, and the in-field experiments demonstrated the superior properties and performances of the developed nanoformulations to control Asian soybean rust and corn helminthosporiosis. Furthermore, these nanoformulations promoted a reduction in the quantities of both AI for pest control in order to reach sustainable agriculture through the decrease in the negative effects from agricultural practices on the environment and public health.

## ■ ASSOCIATED CONTENT

### SI Supporting Information

The Supporting Information is available free of charge at <https://pubs.acs.org/doi/10.1021/acssuschemeng.4c09620>.

Table S1: experimental parameters for  $^{31}\text{P}$  NMR. Figure S1: calibration curve for TBZ quantification by HPLC. Figure S2: calibration curve for PTZ quantification by HPLC (PDF)

## ■ AUTHOR INFORMATION

### Corresponding Author

**Silvio Vaz Júnior** – Brazilian Agricultural Research Corporation, (Embrapa), Brasília, DF 70770-901, Brazil; Graduate Program in Environmental Engineering, Federal University of Ouro Preto, Campus Universitário Morro do Cruzeiro, Ouro Preto, MG 35400-000, Brazil; [orcid.org/0000-0001-8872-4182](https://orcid.org/0000-0001-8872-4182); Email: [silvio.vaz@embrapa.br](mailto:silvio.vaz@embrapa.br)

### Authors

**Flávia Galarza** – Brazilian Agricultural Research Corporation, (Embrapa), Brasília, DF 70770-901, Brazil

**Gabriela Ciribelli Pompeu** – Brazilian Agricultural Research Corporation, (Embrapa), Brasília, DF 70770-901, Brazil

**Helliomar Pereira Barbosa** – Brazilian Agricultural Research Corporation, (Embrapa), Brasília, DF 70770-901, Brazil

**Angelo Aparecido Barbosa Sussel** – Brazilian Agricultural Research Corporation, (Embrapa), Brasília, DF 70770-901, Brazil

Complete contact information is available at: <https://pubs.acs.org/doi/10.1021/acssuschemeng.4c09620>

### Author Contributions

S.V.J.: The Fórmula-AQ Project coordination, manuscript writing, and submission. F.G: nanoformulations preparation, chemical and physicochemical analyses, and manuscript revision. G.C.P.: FTIR and  $^{31}\text{P}$  NMR measurements. H.P.B.: UV–vis fluorescence measurements. A.A.B.S.: in-field experimental validation and manuscript revision.

### Funding

The Article Processing Charge for the publication of this research was funded by the Coordenacao de Aperfeicoamento de Pessoal de Nivel Superior (CAPES), Brazil (ROR identifier: 00x0ma614).

### Notes

The authors declare no competing financial interest.

## ■ ACKNOWLEDGMENTS

Authors thank FAPDF for the financial support and Embrapa for the facilities. SVJr thanks Suzano Paper & Cellulose for the kraft lignin and Adama Brasil for the isolated active ingredients.

## ■ REFERENCES

- (1) Statista. *Agricultural Chemical Industry – Statistics & Facts*, 2024. <https://www.statista.com/topics/3062/agricultural-chemical-industry/#editorsPicks/> (accessed 20 October 2024).
- (2) Vaz, S., Jr. *Analytical Chemistry Applied to Emerging Pollutants*; Springer Nature: Cham, 2018.
- (3) Vaz, S., Jr. *Sustainable Agrochemistry – A Compendium of Technologies*; Springer Nature: Cham, 2019.
- (4) Huang, T.; Tang, X.; Luo, K.; Wu, Y.; Hou, X.; Tang, S. An overview of graphene-based nanoadsorbent materials for environmental contaminants detection. *TrAC, Trends Anal. Chem.* **2021**, *139*, 116255.
- (5) La Merrill, M. A.; Vandenberg, L. N.; Smith, M. T.; Goodson, W.; Browne, P.; Patisaul, H. B.; Guyton, K. Z.; Kortenkamp, A.; Cogliano, V. J.; Woodruff, T. J.; Rieswijk, L.; Sone, H.; Korach, K. S.; Gore, A. C.; Zeise, L.; Zoeller, R. T. Consensus on the key characteristics of endocrine-disrupting chemicals as a basis for hazard identification. *Nat. Rev. Endocrinol.* **2020**, *16*, 45–57.
- (6) Yussof, S. N. M.; Kamari, A.; Aljafree, N. F. A. A review of materials used as carrier agents in pesticide formulations. *Int. J. Environ. Sci. Technol.* **2016**, *13*, 2977–2994.
- (7) Zheng, L.; Seidi, F.; Liu, Y.; Wu, W.; Xiao, H. Polymer-based and stimulus-responsive carriers for controlled release of agrochemicals. *Eur. Polym. J.* **2022**, *177*, 111432.
- (8) Hack, B.; Egger, H.; Uhlemann, J.; Henriët, M.; Wirth, W.; Vermeer, A. W. P.; Duff, D. G. Advanced agrochemical formulations through encapsulation strategies? *Ch. Ing. Tech.* **2012**, *84* (3), 223–234.
- (9) Iavicoli, I.; Leso, V.; Beezhold, D. H.; Shvedova, A. A. Nanotechnology in agriculture: Opportunities, toxicological implications, and occupational risks. *Toxicol. Appl. Pharmacol.* **2017**, *329*, 96–111.
- (10) Wani, T. A.; Masoodi, F. A.; Baba, W. N.; Ahmad, M.; Rahmanian, N.; Jafari, S. M. Nanoencapsulation of Agrochemicals, Fertilizers, and Pesticides for Improved Plant Production. In *Advances in Phytotechnology*, Ghorbanpour, M.; Wani, S. H., Ed.; Academic Press (imprint), Elsevier: Amsterdam, 2019, pp. 279–298.
- (11) Fraceto, L. F.; Grillo, R.; de Medeiros, G. A.; Scognamiglio, V.; Rea, G.; Bartolucci, C. Nanotechnology in agriculture: Which innovation potential does it have? *Front. Environ. Sci.* **2016**, *4*, 20.
- (12) Machado, T. O.; Grabow, J.; Sayer, C.; de Araújo, P. H. H.; Ehrenhard, M. L.; Wurm, F. R. Biopolymer-based nanocarriers for sustained release of agrochemicals: A review on materials and social science perspectives for a sustainable future of agri- and horticulture. *Adv. Colloid Interface Sci.* **2022**, *303*, 102645.
- (13) Ariyanta, H. A.; Sari, F. P.; Sohail, A.; Restu, W. K.; Septiyanti, M.; Aryana, N.; Fatriasari, W.; Kumar, A. Current roles of lignin for the agroindustry: Applications, challenges, and opportunities. *Int. J. Biol. Macromol.* **2023**, *240*, 124523.
- (14) Vaz Jr, S.; Salvador, C. E. D. Innovative structural modification process of Kraft lignin using continuous-flow regime. *Sustainable Chem. Pharm.* **2023**, *36*, 101273.
- (15) Mogul, M. G.; Akin, H.; Hasirci, N.; Trantolo, D. J.; Gresser, J. D.; Wise, D. L. Controlled release of biologically active agents for purposes of agricultural crop management. *Resour., Conserv. Recycl.* **1996**, *16*, 289–320.
- (16) International Lignin Institute, *Showcases of Efficient Lignin Uses*. <https://www.ili-lignin.com/showcase-of-efficient-lignin-uses.html#showcase1/>, (accessed 20 October 2024).
- (17) Scheufele, F. B.; Modenes, A. N.; Borba, C. E.; Ribeiro, C.; Espinoza-Quinones, F. R.; Bergamasco, R.; Pereira, N. C. Monolayer–multilayer adsorption phenomenological model: Kinetics, equilibrium and thermodynamics. *Chem. Eng. J.* **2016**, *284*, 1328–1341.
- (18) Hu, J.; Zhang, Q.; Lee, D.-J. Kraft lignin biorefinery: A perspective. *Bioresour. Technol.* **2018**, *247*, 1181–1183.
- (19) Bajwa, D. S.; Pourhashem, G.; Ullah, A. H.; Bajwa, S. G. A concise review of current lignin production, applications, products and their environmental impact. *Ind. Crops Prod.* **2019**, *139*, 111526.

(20) Dessbesell, L.; Paleologou, M.; Leitch, M.; Pulkki, R.; Xu, C. Global lignin supply overview and kraft lignin potential as an alternative for petroleum-based polymers. *Renewable Sustainable Energy Rev.* **2020**, *123*, 109768.

(21) Asrar, J.; Ding, Y. *Lignin-based Microparticles for the Controlled Release of Agricultural Actives*, US 9,445,599 B2, United States Patent and Trademark Office, Alexandria. 2016.

(22) Thielemans, W.; Wool, R. P. Lignin esters for use in unsaturated thermosets: Lignin modification and solubility modeling. *Biomacromolecules* **2005**, *6* (4), 1895–1905.

(23) Pang, Y.; Chen, Z.; Zhao, R.; Yi, C.; Qiu, X.; Qian, Y.; Lou, H. Facile synthesis of easily separated and reusable silver nanoparticles/aminated alkaline lignin composite and its catalytic ability. *J. Colloid Interface Sci.* **2021**, *587*, 334–346.

(24) Argyropoulos, D. S.; Pajer, N.; Crestini, C. Quantitative <sup>31</sup>P NMR analysis of lignins and tannins. *JoVE Journal* **2021**, *174*, No. e62696.

(25) Ela, R. C. A.; Tajiri, M.; Newberry, N. K.; Heiden, P. A.; Ong, R. G. Double-shell lignin nanocapsules are a stable vehicle for fungicide encapsulation and release. *ACS Sustainable Chem. Eng.* **2020**, *8* (46), 17299–17036.

(26) Pavan, R. V. R.; Barron, A. R. *LibreTexts Chemistry - 2.5: Zeta Potential Analysis*. [https://chem.libretexts.org/Bookshelves/Analytical\\_Chemistry/Physical\\_Methods\\_in\\_Chemistry\\_and\\_Nano\\_Science\\_\(Barron\)/02%3A\\_Physical\\_and\\_Thermal\\_Analysis/2.05%3A\\_Zeta\\_Potential\\_Analysis/](https://chem.libretexts.org/Bookshelves/Analytical_Chemistry/Physical_Methods_in_Chemistry_and_Nano_Science_(Barron)/02%3A_Physical_and_Thermal_Analysis/2.05%3A_Zeta_Potential_Analysis/) (accessed 20 October 2024).

(27) Jeevanandam, J.; Chan, Y. S.; Danquah, M. K. Nanoformulations of drugs: Recent developments, impact and challenges. *Biochimie* **2016**, *128–129*, 99–112.

(28) Machado, T. O.; Beckers, S. J.; Fischer, J.; Müller, B.; Sayer, C.; de Araújo, P. H. H.; Landefester, K.; Wurm, F. R. Bio-based lignin nanocarriers loaded with fungicides as a versatile platform for drug delivery in plants. *Biomacromolecules* **2020**, *21* (7), 2755–2763.

(29) Godoy, C. V.; Seixas, C. D. S.; Soares, R. M.; Marcelino-Guimarães, F. C.; Meyer, M. C.; Costamilan, L. M. Asian soybean rust in Brazil: Past, present, and future. *Pesq. Agropec. Bras.* **2016**, *51* (5), 407–421.

(30) Brasil, S., *Bipolaris e Helminthosporiose: Milho e a Nova Dinâmica de Doenças [Bipolaris and Helminthosporiosis: Corn and the New Disease Dynamics]*. <https://maisagro.syngenta.com.br/dia-a-dia-do-campo/bipolaris-e-helminthosporiose-milho-e-a-nova-dinamica-de-doencas/>. (accessed 20 October 2024).

(31) El Khaldi-Hansen, B.; Schulze, M.; Kamm, B. Qualitative and Quantitative Analysis of Lignins from Different Sources and Isolation Methods for an Application as a Biobased Chemical Resource and Polymeric Material. In *Analytical Techniques and Methods for Biomass*, Vaz Jr, S., Ed.; Springer Nature, Cham, 2016 pp. 15–44.

(32) Pu, Y.; Cao, S.; Ragauskas, A. J. Application of quantitative <sup>31</sup>P NMR in biomass lignin and biofuel precursors characterization. *Energy Environ. Sci.* **2011**, *4*, 3154–3166.

(33) Takada, M.; Okazaki, Y.; Kawamoto, H.; Sagawa, T. Tunable light emission from lignin: Various photoluminescence properties controlled by the lignocellulosic species, extraction method, solvent, and polymer. *ACS Omega* **2022**, *7* (6), 5096–5103.

(34) Zhang, X.; sAbushammala, H.; Puglia, D.; Lu, B.; Xu, P.; Yang, W.; Ma, P. One-step to prepare lignin based fluorescent nanoparticles with excellent radical scavenging activity. *J. Renewable Mater.* **2024**, *12* (5), 895–908.

(35) Huang, C.; Ma, J.; Zhang, W.; Huang, G.; Yong, Q. Preparation of lignosulfonates from biorefinery lignins by sulfomethylation and their application as a water reducer for concrete. *Polymers* **2018**, *10*, 841.

(36) Beckers, S.; Peil, S.; Wurm, F. R. Pesticide-loaded nanocarriers from lignin sulfonates—a promising tool for sustainable plant protection. *ACS Sustainable Chem. Eng.* **2020**, *8* (50), 1846–18475.

(37) Wang, J.; Xiong, Z.; Fan, Y.; Wang, H.; An, C.; Wang, B.; Li, X.; Wang, Y.; Wang, Y. Lignin/surfactin cocervate as an eco-friendly pesticide carrier and antifungal agent against phytopathogen. *ACS Nano* **2024**, *18*, 22415–22430.